ELSEVIER

Chemical Physics 270 (2001) 415–428

Chemical Physics

www.elsevier.com/locate/chemphys

Theoretical studies on the potential energy surface and rovibrational states for the electronic ground state of carbonyl sulfide

Daiqian Xie *, Yuhui Lu, Dingguo Xu, Guosen Yan

Department of Chemistry, Sichuan University, Chengdu 610064, China

Received 10 October 2000

Abstract

A potential energy surface for the electronic ground state of carbonyl sulfide was optimized by using a self-consistent field-configuration interaction method and involving the recent observed vibrational band origins up to 8000 cm^{-1} for the Σ state. The root mean square error for this refinement was found to be 0.27 cm^{-1}. The calculated quartic force constants from the refined potential are very close to the recent high level ab initio calculations. The vibrational energy levels for the Π and Δ states and for some isotopomers of carbonyl sulfide molecule were calculated to test the refined potential. The calculated energy levels are in good agreement with the experimental values.

1. Introduction

Carbonyl sulfide (OCS) plays a very important role in atmospheric and interstellar chemistry. It is the most abundant sulfur-containing species in the troposphere of the earth [1] and has been observed in several molecular cloud sources in the interstellar medium by radioastronomy [2,3]. Recently, the potential energy surface (PES) and the rovibrational spectra of OCS have been studied extensively by experimental [4–12] and theoretical techniques [13–20]. The study of vibrational spectra of this molecule started early in 1932 [21], and since then it has been extensively investigated. Now, it has been well established that OCS is a linear molecule at the equilibrium geometry with C–S distance of 1.5614 Å and C–O distance of 1.1562 Å [6] for its electronic ground state. The molecule is very stable with a dissociation energy of ~73.2 cal mol^{-1} [18]. It was shown that the normal mode picture is appropriate in describing the low-lying vibrational levels of this molecule [12]. This is consistent with the relatively small mass disparities among the constituent atoms. More recently, highly excited vibrational levels have been systematically investigated using the Fourier transform spectrometer and the laser photoacoustic techniques [9–12], which provide a new global rovibrational analysis and useful information about the PES of the OCS molecule.

Most of the theoretical studies on this molecule have concentrated on the ground electronic

* Corresponding author. Fax: +86-28-541-2907.
E-mail address: dqxie@scu.edu.cn (D. Xie).

0301-0104/01/$ - see front matter
PII: S0301-0104(01)00406-2

state, although some work on excited state has been reported [19]. Morino and Nakagawa [13] determined at first the anharmonic force field by using a least-squares analysis based on the second-order perturbation theory. That force field was refined by Foord et al. [14] via the numerical solution of the vibrational Hamiltonian matrix and iterative least-squares adjustment. Steele et al. [15] calculated the force field with the 4-31G basis set at Hatree–Fock level. Peterson and coworkers [16] calculated the stretching PES of this system at MP4 and CISD levels. Using the calculated PES, they also computed the spectroscopic constants and stretching band origins up to 6000 cm^{-1}. Due to the neglect of the stretch–bend interactions, their results are somewhat overestimated compared with the experimental values. More recently, Martin et al. [17] and Pak and Woods [18] studied the force field of OCS at CCSD(T)/cc-pvtz level and CCSD(T)/cc-pvqz level, respectively. Although these PESs could be used to study the harmonic vibration and low-exciting vibrational levels, they are not accurate enough to predict the highly excited rovibrational levels of OCS.

The major motive of this paper is to generate a refined near equilibrium PES which could reproduce highly excited rovibrational levels of OCS well. To this end, we used the self-consistent field-configuration interaction (SCF-CI) method [22] to optimize the PES of OCS. The remainder of the paper is organized as follows. Section 2 discusses the fitting method of the potential energy surface and the assignment of the energy levels. The calculated results presented in Section 3 include the PES and vibrational energy levels.

2. Computational details

2.1. Fitting potential energy surface from experimental frequencies

In a theoretical study of the rovibrational states for a triatomic molecule, the potential energy function is often written as a power series expansion of suitable coordinates. In the present work, the Morse-cosine expansion [23] is used as the analytical representation of the potential function:

$$V(r_1, r_2, \theta) = \sum_{ijk} f_{ijk} y_1^i y_2^j y_3^k, \tag{1}$$

where r_1 and r_2 are bond lengths, θ is the enclosed angle, and the quantities y_l are defined as:

$$y_l = 1 - \exp[-\alpha_l(r_l - r_{le})], \quad l = 1, 2, \tag{2}$$

$$y_3 = \cos\theta - \cos\theta_e, \tag{3}$$

where the α_l is the Morse exponential parameter and r_{le} is the equilibrium value of r_l. For the OCS molecule, we defined α_1 and r_1 corresponding to the C–S bond while α_2 and r_2 corresponding to the O–C bond.

In this work, the computer program SCFCI has been used in the calculation. The SCF-CI methodology, described in detail in Ref. [24], involves a variational calculation of the rovibrational term values directly from the PES. In the least-squares fitting procedure that is built into the program, the parameters describing the PES can be varied to optimize the differences between the experimental and variationally derived term values. In the procedure, the optimized parameters in the potential energy function can be obtained by minimizing the weighted least-squares objective function defined by:

$$F = \sum_n \left[\omega_n \left(E_n^{(\mathrm{obs})} - E_n^{(\mathrm{cal})}\right)\right]^2, \tag{4}$$

where the summation runs over all the observed rovibrational states of interest, ω_n is the weighting coefficient for rovibrational state n, $E_n^{(\mathrm{obs})}$ is the observed rovibrational energy level and $E_n^{(\mathrm{cal})}$ is the calculated level obtained using a variational procedure. The optimizer Levenberg–Marguardt–Fletcher (LMF) can be used to minimize the least-squares objective function. The derivatives of the calculated rovibrational energies with respect to the parameters in the potential energy function $\partial E_n/\partial P$ (where P denotes to any one of the parameters) can be calculated using the Hellmann–Feynman theorem:

$$\frac{\partial E_n}{\partial P} = \left\langle \psi_n \left| \frac{\partial V}{\partial P} \right| \psi_n \right\rangle. \tag{5}$$

2.2. Calculating vibrational energy levels via discrete variable representation and Lanczos iteration

For the OCS system with zero total angular momentum, the vibrational Hamiltonian is given below in the Radau coordinate,

$$H = -\frac{1}{2m_a}\frac{\partial^2}{\partial R_1^2} - \frac{1}{2m_c}\frac{\partial^2}{\partial R_2^2} - \left(\frac{1}{2m_a R_1^2} + \frac{1}{2m_c R_2^2}\right) \times \left(\frac{\partial^2}{\partial\theta^2} + \cot\theta\frac{\partial}{\partial\theta}\right) + V(R_1, R_2, \theta), \tag{6}$$

where m_a and m_c are the mass of S and O atom, respectively. The use of Radau coordinates simplifies the kinetic energy operator while preserving the molecular symmetry. The transformation of the Radau coordinates (R_1, R_2, θ) to internal coordinates is well-documented [25]. In this work, we used in the calculation a three-dimensional direct-product discrete variable representation (DVR). The Hamiltonian matrix expressed in the direct-product DVR is very sparse:

$$H_{ijk,i'j'k'} = T^1_{i,i'}\delta_{jj'}\delta_{kk'} + T^2_{j,j'}\delta_{ii'}\delta_{kk'} + \left(\frac{1}{2m_a R_{1i}^2} + \frac{1}{2m_c R_{2j}^2}\right)\delta_{ii'}\delta_{jj'}T^3_{k,k'} + \delta_{ii'}\delta_{jj'}\delta_{kk'}V(R_{1i}, R_{2j}, \theta_k). \tag{7}$$

The direct-product DVR is memory efficient since only the diagonal potential matrix and three small kinetic energy matrices need to be stored. Apparently, the major computational expense is in calculating the action of kinetic energy operators. The efficiency of $H\Psi$ can be significantly improved if dimensions of the kinetic energy matrices can be reduced. One way to achieve this is to use PODVR method [26], where the DVR points are placed according to the PES. The PODVR method takes the advantage of including some information about the PES to reduce the number of DVR points. This is done by using the eigenfunctions of convenient one-dimensional reference Hamiltonian as the basis sets. The PODVR method has been proved to be much more efficient than the usual DVR method [26,27].

Since the Hamiltonian matrix expressed in the PODVR is very sparse, the Lanczos algorithm [28] can be used to diagonize the matrix. As an iterative method, the Lanczos algorithm generates a series of orthonormal Lanczos states via a three-term iterative formula. From a normalized initial state $|\varphi_1\rangle$ which is chosen arbitrarily, a series of Lanczos states can be generated with the iterative scheme $(m = 1, 2, \ldots, M)$,

$$\begin{aligned} |\varphi_{m+1}\rangle &= (H|\varphi_m\rangle - \alpha_m|\varphi_m\rangle - \beta_{m-1}|\varphi_{m-1}\rangle)/\beta_m, \\ \alpha_m &= \langle\varphi_m|H|\varphi_m\rangle, \\ \beta_m &= \|H|\varphi_m\rangle - \alpha_m|\varphi_m\rangle - \beta_{m-1}|\varphi_{m-1}\rangle\|, \\ \beta_0 &= 0. \end{aligned} \tag{8}$$

Apparently, the Lanczos algorithm has a minimal storage requirement. The Hamiltonian on the Lanczos bases assumes the tridiagonal form (the Lanczos matrix) and its diagonalization yields the eigenvalues. In the Lanczos approach, one can always obtain some information related to the eigenvalues and eigenstates at any steps, thanks to its iterative nature. The information may not be accurate if the number of iterations is not large enough, but one always gains something useful. As more iterations carried out, the information generally becomes more accurate.

A problem associated with the Lanczos algorithm in finite precision arithmetic is the loss of global orthogonality among the Lanczos states, which results in the emergence of spurious eigenvalues. Although the deterioration of orthogonality is partially due to round-off errors, it has been shown that it is also related to the convergence of certain eigenvalues [29,30]. The orthogonality of the Lanczos states can be restored by forced orthogonalizations, but it is computationally expensive. In this work, we used a simple and reliable method suggested by Cullum and Willoughby [31] to eliminate the spurious eigenvalues.

2.3. Assignment of vibrational levels

The assignment of the calculated energy levels with three quantum numbers $(v_1\, v_2\, v_3)$ for the suitable independent modes is usually a demanding task. The numbers v_1, v_2, and v_3 refer to the CS

stretching mode, the bending mode and the OC stretching mode, respectively. The assignment is sometimes not unique especially for the highly excited vibrational states, because of the significant anharmonic coupling. In this work, we at first calculated the following three quantities for a specific vibrational state n,

$$\begin{aligned} Q_{1n} &= \langle\psi_n|(r_1 - r_{1e})^2|\psi_n\rangle, \\ Q_{2n} &= \langle\psi_n|(\cos\theta - \cos\theta_e)^2|\psi_n\rangle, \\ Q_{3n} &= \langle\psi_n|(r_2 - r_{2e})^2|\psi_n\rangle. \end{aligned} \tag{9}$$

The three above integrals can be calculated using directly the eigenfunction obtained from a variational calculations, or using the perturbation method suggested by Ma et al. [32] without calculating and storing the eigenstates. The values of Q_{1n}, Q_{2n}, and Q_{3n} provide useful information about the eigenstate. If the vibrational state is harmonic, the quantity Q_{kn} $(k = 1, 2, 3)$ has a linear relation with the quantum number v_k. This assignment is trivial for the lowly excited vibrational levels. With the increase of the vibrational energy, intermodal couplings typically strengthen and the separability of the vibrational modes becomes less satisfactory. It is particularly true for systems undergoing normal to local mode transitions [33]. Despite these difficulties, useful information can still be extracted. This prescreening procedure allows us to identify the likely candidates for the states of interest with a relatively small numerical price. The final assignments of vibrational states could be carried out by combining this information with the energy differences and the nodal structures of the wave functions.

3. Results

The recent ab initio force constants of Pak and woods [18] were taken as the initial guess for the PES. At first, we performed an SCF calculation on the vibrational ground state by solving the stretching one-dimensional SCF equations using the renormalized Numerov method of Johnson [34] with 3000 sectors in the region of 2.0–5.0 bohr for O–S stretching, and 1.6–4.5 bohr for O–C stretching; and solving the bending one-dimensional SCF equation variationally with 150 Legendre polynomials as the basis function. Then, we carried out CI calculations with two sets which took 5500 and 6000 lowest configurations, respectively. This test showed that the CI calculation with 5500 configurations converged all band origins below 8000 cm^{-1} to 0.01 cm^{-1} or better, compared with the results obtained with 6000 configurations. Thus, all subsequent CI calculations required in the optimization were performed with 5500 configurations.

In the optimization of the potential parameters appeared in Eq. (1), the 93 vibrational band origins up to 8000 cm^{-1} were used as the input data points. Besides the 50 observed vibrational band origins from a number of recent experiments [5–11], we involved the 43 vibrational band origins from the effective Hamiltonian derived by Fayt and coworkers [9]. This effective Hamiltonian contains a set of 148 molecular parameters, and a statistical agreement is obtained with all the available experimental data. It is expected [35] that the accuracy is better than 0.1 cm^{-1} even in the worst cases. The weighting coefficients ω_n in the least-squares objective function (4) were taken to be 1.0 for all the band origins. The equilibrium geometry of OCS was fixed at the observed values [6]: $r_{1e} = 1.5614$ Å, $r_{2e} = 1.1562$ Å, and $\theta_e = 180°$.

The optimized parameter values of the PES for OCS are given in Table 1. In Fig. 1, we present the contour plots of the refined PES of OCS in valence coordinates, with the angular and radial coordinates fixed at their equilibrium values respectively. As observed, the PES is well behaved even for large values of the vibrational coordinates. In Table 2, the 93 observed vibrational band origins are listed together with the calculated vibrational band origins in the final fittings. It can be seen from this table that the refined PES of this work can reproduce well the 93 observed vibrational band origins. The corresponding root mean square (RMS) error is 0.27 cm^{-1}. Most calculated band origins are within 0.5 cm^{-1} of the observed values. The maximum deviation of the calculated results from the observed values is -0.85 cm^{-1} for the

Table 1
Values of the parameters of the potential energy function for OCS[a]

ijk	F_{ijk} (cm^{-1})	ijk	F_{ijk} (cm^{-1})
001	32849.58	002	15623.64
011	−17553.99	020	72972.84
101	−27625.23	110	9857.17
200	50043.09	300	−2376.30
400	336.49	003	4971.79
012	−3360.94	021	−8550.95
030	−64.84	102	−4597.25
111	18285.40	120	−657.28
201	−7181.44	210	1985.36
004	2553.25	013	−5546.12
022	−4905.39	031	−11098.50
040	3505.21	103	−9178.03
112	−21854.86	121	948.74
130	−1416.44	202	−983.04
211	5596.86	220	−584.78
301	−142.39	310	1694.77

[a] See Eq. (1) for the form of the potential. The values of the equilibrium bond lengths r_{1e} and r_{2e} were fixed at their observed values [6] ($r_{1e} = 1.5614$ Å, $r_{2e} = 1.1562$ Å, $\theta_e = 180°$, $\alpha_1 = 1.95$ $Å^{-1}$, $\alpha_2 = 2.34$ $Å^{-1}$).

vibrational state (9 0 0), whereas the corresponding deviation of the calculated levels obtained from the empirical potential of Zuniga et al. [20] is found to be -3.2 cm^{-1}.

In Table 3, the values of the force constants defined as the derivatives of $V(r_1, r_2, \theta)$ (Eq. (1)) at equilibrium are given together with those of Foord et al. [14], Peterson et al. [16], Martin et al. [17], Pak and Woods [18] and Zuniga et al. [20]. It can be seen from Table 3 that all the force constants obtained in this work are in better agreement with the ab initio results, compared with a former fitted force field by Zuniga et al. [20]. For example, for force constant f_{rrrR}, the present result is 2.632 aJ $Å^{-4}$, and the ab initio values are 2.731 aJ $Å^{-4}$ [17] and 2.557 aJ $Å^{-4}$ [18], whereas that of Zuniga's fitting is -0.465 aJ $Å^{-4}$. This also shows the good behavior of our fitted PES.

In order to test the refined potential, we calculated the vibrational energy levels for some isotopomers of the OCS molecule using the optimized PES and listed the results in Table 4, compared with the observed vibrational energy levels [6,11]. From Table 4, one can see that the optimized PES

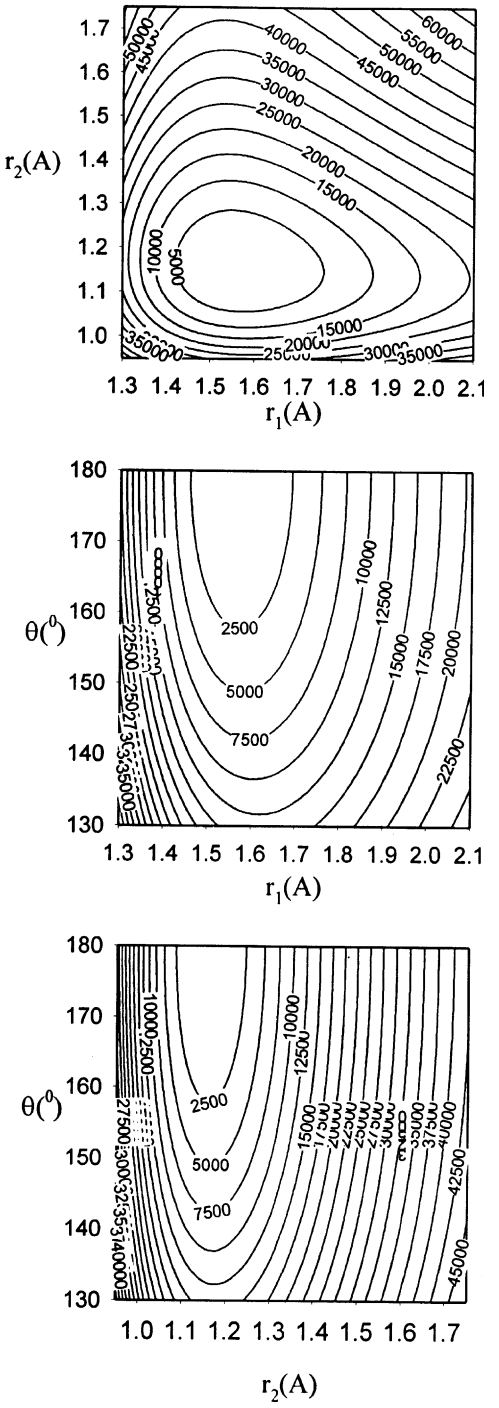

Fig. 1. Contour plots of the fitted PES (in cm^{-1}) of OCS. The θ (upper), r_2 (middle), and r_1 (lower) are fixed at their equilibrium values, respectively.

Table 2
Comparison between observed and calculated vibrational frequencies (cm^{-1}) for Σ state of OCS

$(v_1\, v_2\, v_3)$	E_n^{obs}	$E_n^{obs} - E_n^{cal}$	$(v_1\, v_2\, v_3)$	E_n^{obs}	$E_n^{obs} - E_n^{cal}$
(1 0 0)	858.97 [8]	0.03	(0 2 0)	1047.04 [36]	−0.02
(2 0 0)	1710.98 [5]	0.12	(1 2 0)	1892.23 [5]	−0.20
(0 0 1)	2062.20 [5]	0.21	(0 4 0)	2104.83 [5]	0.11
(3 0 0)	2555.99 [5]	0.24	(2 2 0)	2731.40 [5]	−0.27
(1 0 1)	2918.11 [7]	0.19	(1 4 0)	2937.15 [7]	−0.05
(0 2 1)	3095.55 [5]	0.25	(0 6 0)	3170.64 [7]	0.22
(4 0 0)	3393.97 [7]	0.37	(3 2 0)	3564.48 [7]	−0.28
(2 4 0)	3762.83 [10]	−0.10	(2 0 1)	3768.50 [10]	0.21
(1 2 1)	3937.43 [10]	−0.02	(1 6 0)	3990.11 [7]	0.14
(0 0 2)	4101.39 [10]	0.16	(0 4 1)	4141.21 [10]	0.31
(5 0 0)	4224.87 [10]	0.46	(0 8 0)	4242.55 [7]	0.24
(4 2 0)	4391.41 [7]	−0.25	(3 4 0)	4585.25 [10]	−0.17
(3 0 1)	4609.85 [10]	0.36	(2 2 1)	4773.22 [10]	−0.18
(2 6 0)	4805.16 [5]	0.08	(1 0 2)	4953.88 [10]	0.09
(1 4 1)	4970.43 [10]	0.03	(6 0 0)	5048.62[a]	0.45
(1 8 0)	5049.14[a]	0.26	(0 2 2)	5120.98 [10]	0.30
(0 6 1)	5196.01 [10]	0.24	(5 2 0)	5212.14[a]	−0.21
(0 10 0)	5319.02[a]	0.12	(4 4 0)	5401.48[a]	−0.14
(4 0 1)	5444.96 [10]	0.47	(3 2 1)	5602.47 [10]	−0.21
(3 6 0)	5616.07[a]	0.07	(2 4 1)	5792.00 [10]	−0.19
(2 0 2)	5801.91 [9]	0.18	(2 8 0)	5852.00[a]	0.28
(7 0 0)	5865.18[a]	0.31	(1 2 2)	5959.33 [9]	−0.08
(1 6 1)	6012.06[a]	0.05	(6 2 0)	6026.59[a]	−0.19
(1 10 0)	6112.59[a]	0.25	(0 0 3)	6117.58 [9]	−0.09
(0 4 2)	6154.70 [9]	0.29	(5 4 0)	6212.12[a]	−0.09
(0 8 1)	6257.83[a]	0.03	(5 0 1)	6273.13 [8]	0.57
(0 12 0)	6398.77[a]	−0.13	(4 6 0)	6418.68 [8]	0.17
(4 2 1)	6429.10 [8]	−0.25	(3 4 1)	6611.11 [8]	−0.25
(3 0 2)	6640.10 [9]	0.26	(3 8 0)	6650.90[a]	0.29
(8 0 0)	6674.46[a]	−0.06	(2 2 2)	6791.54 [9]	−0.32
(2 6 1)	6823.87[a]	−0.05	(7 2 0)	6834.69[a]	−0.26
(2 10 0)	6903.16[a]	0.32	(1 0 3)	6966.17 [9]	−0.19
(1 4 2)	6980.96 [9]	−0.09	(6 4 0)	7017.13[a]	−0.04
(1 8 1)	7060.66[a]	0.01	(6 0 1)	7094.22[a]	0.55
(0 2 3)	7123.38 [9]	0.16	(1 12 0)	7179.14[a]	0.05
(0 6 2)	7198.75[a]	0.08	(5 6 0)	7220.13[a]	0.27
(5 2 1)	7245.75[a]	−0.31	(0 10 1)	7324.96[a]	−0.31
(4 4 1)	7423.79[a]	−0.18	(4 8 0)	7445.74[a]	0.24
(4 0 2)	7472.18 [9]	0.36	(9 0 0)	7476.38[a]	−0.85
(0 14 0)	7480.69[a]	−0.54	(3 2 2)	7616.85 [8]	−0.40
(3 6 1)	7631.94[a]	−0.13	(8 2 0)	7636.35[a]	−0.49
(3 10 0)	7690.33[a]	0.33	(2 4 2)	7797.96[a]	−0.49
(2 0 3)	7811.95 [9]	−0.04	(7 4 0)	7816.43[a]	−0.05
(2 8 1)	7859.95[a]	−0.01	(7 0 1)	7908.22[a]	0.36
(2 12 0)	7957.27[a]	0.11	(1 2 3)	7958.04[a]	−0.30
(1 6 2)	8011.27[a]	−0.21	(6 6 0)	8015.70[a]	0.32
(6 2 1)	8057.05[a]	−0.34	RMS		0.27

[a] Calculated values from the effective Hamiltonian derived by Fayt and coworkers [9].

of $^{16}O\,^{12}C\,^{32}S$ can reproduce the vibrational energy levels of its isotopomers well. In addition, we used the two-step procedure [24] to calculate the ro-vibrational energy levels of $^{16}O\,^{12}C\,^{32}S$ (for $J \leqslant 3$)

Table 3
Comparison between the quartic internal coordinate force constants (aJ; Å; Rad) of the ab initio and empirical potentials for OCS

	MP4SDQ [16]	Experimental [14]	CCSD(T) [17]	CCSD(T) [18]	Fitted [20]	This work
f_{rr}	16.198	16.009	16.028	16.123	16.048	15.875
f_{rR}	1.087	0.986	0.938	1.009	0.9904	0.893
f_{RR}	7.486	7.510	7.338	7.407	7.4982	7.560
$f_{\theta\theta}$	0.653	0.649	0.651	0.655	0.6518	0.653
f_{rrr}	−116.193	−95.166	−111.894	−113.191	−111.891	−111.540
f_{rrR}	−2.796	−3.472	−2.583	−2.670	−2.549	−2.370
f_{rRR}	−1.541	0.64	−0.969	−1.170	−2.633	−1.040
f_{RRR}	−44.026	−46.524	−43.234	−43.355	−44.944	−46.327
$f_{r\theta\theta}$		−3.092	−0.808	−0.821	−0.876	−0.816
$f_{R\theta\theta}$		−0.308	−0.977	−0.964	−1.167	−1.070
f_{rrrr}	689.683	317.064	654.122	669.240	619.833	659.960
f_{rrrR}	−1.488		2.731	2.557	−0.465	2.632
f_{rrRR}	1.603		2.364	2.704	4.441	2.011
f_{rRRR}	3.523		3.450	3.820	7.766	2.797
f_{RRRR}	198.110	205.152	191.343	192.971	216.089	228.121
$f_{rr\theta\theta}$		11.096	0.032	0.127	−0.330	0.049
$f_{rR\theta\theta}$			1.010	1.686	1.446	1.657
$f_{RR\theta\theta}$		0.885	0.567	0.781	0.236	1.002
$f_{\theta\theta\theta\theta}$		2.163	2.734	1.169	1.639	1.210

with this PES. In the first step, we solved a series of vibrational problems, defined by neglecting Coriolis coupling in the exact rovibrational Hamiltonian, using the SCF-CI method to produce the eigenfunctions and eigenvalues with 5500 configurations. In the second step, we took the 500 lowest eigenfunctions obtained in the first step to construct and diagonalize the exact rovibrationl Hamiltonian matrix in the bond length–bond angle coordinates for the total angular momentum $J \leqslant 3$. The band origins of Π state and Δ state vibration are listed in Tables 5 and 6 together with the values obtained from the observed rovibrational spectra [8–10]. The band origins of Π state and Δ state vibration are generated with the formula:

$$B_v = \frac{E(v,J+1) - E(v,J)}{2J+2}, \qquad G_v = E(v,J) - B_v J(J+1). \tag{10}$$

It can be seen from Tables 5 and 6 that the calculated band origins of Π state and Δ state vibration are in good agreement with the observed values. This shows that the refined potential of OCS may be used to study the vibrational states and rovibrational states for lower J to a reasonable accuracy.

Fig. 2 displays several contour plots of the pure vibrational states (4 0 0), (3 0 1), (6 0 0), (5 0 1), (8 0 0) and (7 0 1) (where the quantum number $l = 0$), with the bond angle fixed at its equilibrium value. From the Fig. 2 one can see that the wave functions show a systematic and characteristic change in their nodal patterns when energy increases. For relatively low v_1, the vibration is largely normal in the sense that the wave function is basically along the C–S stretching coordinate. However, as v_1 increases, the wave function exhibit erratic nodal structure: the nodal lines are no longer parallel to each other, and the coupling between C–S and C–O stretching vibrations is significant. Fig. 3 shows the wave function of vibrational states (1 4 0), (0 4 1), (1 6 0), (0 6 1), (1 8 0) and (0 8 1). One can see from Fig. 3 that the low excited vibrational states such as (1 4 0) and (0 4 1) have regular nodal structures, which implies that, at low energy region, both the C–S (v_1) and C–O (v_3) stretching vibration have a comparative weak interaction with bending vibration (v_2). While for higher excited states, the couplings between

Table 4
Differences between the calculated and observed vibrational frequencies (cm^{-1}) for some isotopomers of OCS[a]

OCS (18-12-34)			OCS (17-12-32)			OCS (18-13-32)		
(ijk)	E_n^{obs}	$E_n^{obs} - E_n^{cal}$	(ijk)	E_n^{obs}	$E_n^{obs} - E_n^{cal}$	(ijk)	E_n^{obs}	$E_n^{obs} - E_n^{cal}$
(1 0 0)	826.65	0.29	(1 0 0)	848.14	0.18	(1 0 0)	834.38	0.13
(0 2 0)	1034.32	−0.04	(0 2 0)	1041.32	−0.02	(0 2 0)	1005.11	0.01
(2 0 0)	1647.16	0.66	(2 0 0)	1689.61	0.42	(2 0 0)	1662.27	0.43
(1 2 0)	1847.99	0.06	(1 2 0)	1875.80	−0.05	(1 2 0)	1826.00	−0.08
(0 0 1)	2025.32	−0.37	(0 0 1)	2043.08	−0.14	(0 0 1)	1971.80	−0.11
(0 4 0)	2079.06	0.07	(0 4 0)	2093.45	0.12	(0 4 0)	2020.80	0.09
(3 0 0)	2461.39	1.00	(3 0 0)	2524.36	0.68	(3 0 0)	2483.34	0.56
(2 2 0)	2656.31	0.23	(2 2 0)	2704.52	0.01	(2 2 0)	2641.21	−0.08
(1 0 1)	2848.47	−0.10	(1 0 1)	2887.96	0.01	(1 0 1)	2803.37	−0.02
(1 4 0)	2880.45	0.17	(1 4 0)	2915.09	0.09	(1 4 0)	2829.25	0.13
(0 2 1)	3045.91	−0.31	(0 2 1)	3070.75	−0.07	(0 2 1)	2964.43	−0.01
(0 6 0)	3131.84	0.16	(0 6 0)	3153.73	0.23	(0 6 0)	3044.49	0.17
(4 0 0)	3269.36	1.35	(4 0 0)	3352.38	0.95	(4 0 0)	3298.22	1.12
(3 2 0)	3459.20	0.46	(3 2 0)	3527.45	0.17	(3 2 0)	3451.02	0.32
(2 0 1)	3665.38	0.17	(3 0 1)	3725.78	0.19	(2 0 1)	3627.78	0.09
(2 4 0)	3677.31	0.36	(2 4 0)	3732.21	0.17	(2 4 0)	3633.35	0.26
(1 2 1)	3855.92	−0.31	(1 2 1)	3901.76	−0.19	(1 2 1)	3782.20	−0.24
(1 6 0)	3921.03	0.33	(1 6 0)	3962.64	0.28	(1 6 0)	3840.52	0.33
(0 0 2)	4028.64	−1.00	(0 0 2)	4063.70	−0.54	(0 0 2)	3922.67	−0.53
OCS (18-12-33)			OCS (17-12-34)			OCS (16-13-34)		
(1 0 0)	832.53	0.66	(1 0 0)	837.04	0.36	(1 0 0)	843.13	−0.19
(0 2 0)	1035.23	−0.03	(0 2 0)	1039.42	−0.04	(0 2 0)	1014.26	−0.03
(2 0 0)	1658.08	0.66	(2 0 0)	1667.27	0.40	(2 0 0)	1679.36	−0.30
(1 2 0)	1854.18	0.07	(1 2 0)	1863.17	−0.06	(1 2 0)	1844.29	−0.41
(0 0 1)	2025.72	−0.41	(0 0 1)	2042.29	−0.06	(0 0 1)	2008.47	0.67
(0 4 0)	2081.10	0.10	(0 4 0)	2089.21	0.06	(0 4 0)	2038.63	0.11
(3 0 0)	2477.65	1.03	(3 0 0)	2491.21	0.66	(3 0 0)	2508.68	−0.38
(2 2 0)	2667.68	0.25	(2 2 0)	2681.34	0.03	(2 2 0)	2668.33	−0.68
(1 0 1)	2854.76	0.23	(1 0 1)	2876.02	0.28	(1 0 1)	2848.75	0.38
(1 4 0)	2887.52	0.18	(1 4 0)	2900.58	0.04	(1 4 0)	2856.89	−0.19
(0 2 1)	3047.27	−0.34	(0 2 1)	3067.97	−0.01	(0 2 1)	3010.03	0.72
(0 6 0)	3135.13	0.22	(0 6 0)	3146.92	0.13	(0 6 0)	3070.47	0.25
(4 0 0)	3290.87	1.43	(4 0 0)	3308.60	0.92	(4 0 0)	3331.07	−0.47
(3 2 0)	3475.72	0.52	(3 2 0)	3493.86	0.19	(3 2 0)	3486.35	−0.88
(2 0 1)	3676.77	0.17	(2 0 1)	3702.36	0.21	(2 4 0)	3668.32	−0.56
(2 4 0)	3689.34	0.35	(2 4 0)	3707.71	0.16	(2 0 1)	3683.72	0.34
(1 2 1)	3862.57	−0.32	(1 2 1)	3888.19	−0.14	(1 2 1)	3837.18	0.24
(1 6 0)	3929.14	0.36	(1 6 0)	3945.99	0.19	(1 6 0)	3876.28	−0.07
(0 0 2)	4029.48	−1.05	(0 0 2)	4062.06	−0.40	(0 0 2)	3994.92	1.06

[a] The observed data are taken from Ref. [11].

bending and stretching vibration become significantly strong, this could be seen from the irregular nodal structures of vibrational states (1 6 0) and (1 8 0). It is interesting to note here the intermodal coupling between the bending vibration and C–S stretching vibration is stronger than that of bending–C–O stretching vibration. This should be attributed to the nature of the potential. The coupling parameter F_{101}, which describes the interaction between v_1 and v_2 vibration, has a value of $-27\,625.23$ cm^{-1}, while the corresponding coupling parameter of v_2–v_3 interaction, F_{011}, is

Table 5
Comparison between observed and calculated vibrational frequencies and effective rotational constants for the Π state of OCS[a]

$(v_1\, v_2\, v_3)$	E_n^{obs} (cm^{-1})	E_n^{cal} (cm^{-1})	B^{obs} (cm^{-1})	B^{cal} (cm^{-1})
(0 1 0)	520.422	520.567	0.20321	0.203
(1 1 0)	1372.459	1372.729	0.20266	0.203
(0 3 0)	1573.366	1573.406	0.20376	0.204
(2 1 0)	2218.029	2218.332	0.20209	0.202
(1 3 0)	2412.122	2412.359	0.20326	0.203
(0 1 1)	2575.308	2575.182	0.20202	0.202
(0 5 0)	2635.590	2635.482	0.20420	0.204
(3 1 0)	3057.094	3057.367	0.20151	0.201
(2 3 0)	3245.261	3245.594	0.20274	0.203
(1 1 1)	3424.140	3424.219	0.20152	0.201
(1 5 0)	3461.579	3461.611	0.20370	0.204
(0 3 1)	3615.345	3615.127	0.20262	0.203
(0 7 0)	3704.772	3704.588	0.20456	0.205
(4 1 0)	3889.613	3889.826	0.20091	0.201
(3 3 0)	4072.694	4073.048	0.20222	0.202
(2 1 1)	4266.325	4266.509	0.20107	0.201
(2 5 0)	4282.908	4282.997	0.20313	0.203
(1 3 1)	4450.760	4450.865	0.20216	0.202
(1 7 0)	4517.943	4517.792	0.20407	0.204
(0 1 2)	4607.109	4606.959	0.20083	0.201
(0 5 1)	4666.093	4665.864	0.20308	0.203
(5 1 0)	4715.537	4715.694	0.20030	0.200
(0 9 0)	4779.227	4779.082	0.20486	0.205
(4 3 0)	4894.345	4894.671	0.20167	0.202
(3 5 0)	5097.045	5097.169	0.20239	0.203
(3 1 1)	5104.231	5104.403	0.20076	0.201
(2 3 1)	5280.540	5280.836	0.20170	0.202
(2 7 0)	5327.027	5326.877	0.20357	0.204
(1 1 2)	5452.463	5452.590	0.20040	0.200
(1 5 1)	5488.783	5488.815	0.20259	0.203
(6 1 0)	5534.805	5534.952	0.19966	0.200
(1 9 0)	5579.462	5579.236	0.20436	0.205
(0 3 2)	5634.235	5633.989	0.20149	0.202
(5 3 0)	5710.144	5710.419	0.20111	0.201
(0 7 1)	5724.781	5724.679	0.20349	0.204
(0 11 0)	5857.567	5857.600	0.20510	0.206
(4 5 0)	5908.976	5909.024	0.20223	0.202
(4 1 1)	5932.727	5932.908	0.19985	0.200
(3 3 1)	6104.517	6104.883	0.20126	0.201
(3 7 0)	6131.881	6131.725	0.20302	0.203
(2 1 2)	6290.913	6291.221	0.20011	0.200
(2 5 1)	6307.119	6307.283	0.20194	0.202
(7 1 0)	6347.345	6347.578	0.19900	0.199
(2 9 0)	6376.316	6376.036	0.20387	0.204
(1 3 2)	6466.146	6466.351	0.20108	0.201
(6 3 0)	6520.018	6520.251	0.20053	0.201
(1 7 1)	6534.399	6534.418	0.20300	0.203
(0 1 3)	6615.854	6615.872	0.19965	0.200
(1 11 0)	6644.695	6644.559	0.20459	0.205
(0 5 2)	6673.761	6673.623	0.20198	0.202
(5 5 0)	6714.772	6714.744	0.20171	0.202
(5 1 1)	6755.610	6755.757	0.19926	0.199
(0 9 1)	6789.568	6789.736	0.20383	0.204

(*continued on next page*)

Table 5 (*continued*)

$(v_1\, v_2\, v_3)$	E_n^{obs} (cm^{-1})	E_n^{cal} (cm^{-1})	B^{obs} (cm^{-1})	B^{cal} (cm^{-1})
(4 3 1)	6921.913	6922.106	0.20112	0.201
(3 9 0)	6933.044	6933.033	0.20217	0.202
(0 13 0)	6938.605	6938.968	0.20529	0.206
(3 5 1)	7116.505	7116.821	0.20144	0.202
(3 1 2)	7126.896	7127.175	0.19966	0.200
(8 1 0)	7153.074	7153.565	0.19832	0.198
(4 7 0)	7169.470	7169.166	0.20337	0.204
(2 3 2)	7292.418	7292.910	0.20067	0.201
(7 3 0)	7323.892	7324.135	0.19993	0.200
(2 7 1)	7340.065	7340.146	0.20251	0.203
(2 11 0)	7429.192	7428.976	0.20409	0.205
(1 1 3)	7457.434	7457.792	0.19930	0.199
(1 5 2)	7493.096	7493.329	0.20149	0.202
(6 5 0)	7515.153	7515.051	0.20117	0.201
(6 1 1)	7572.022	7572.162	0.19865	0.199
(1 9 1)	7585.806	7585.924	0.20332	0.204
(0 3 3)	7630.108	7630.016	0.20037	0.200
(1 13 0)	7712.373	7712.549	0.20472	0.205
(0 7 2)	7722.385	7722.514	0.20248	0.203
(5 7 0)	7725.247	7724.834	0.20205	0.202
(5 3 1)	7737.801	7738.318	0.20020	0.200
(0 11 1)	7858.896	7859.475	0.20412	0.205
(4 5 1)	7925.383	7925.583	0.20133	0.201
(4 1 2)	7951.728	7951.970	0.19886	0.199
(9 1 0)	7951.891	7953.055	0.19761	0.198
(4 9 0)	7958.805	7958.549	0.20278	0.203
(0 15 0)	8021.286	8022.145	0.20543	0.206

[a] The observed values are taken from Fayt and coworkers [9].

Table 6
Comparison between observed and calculated vibrational frequencies and effective rotational constants for the Δ state of OCS[a]

$(v_1\, v_2\, v_3)$	E_n^{obs} (cm^{-1})	E_n^{cal} (cm^{-1})	B^{obs} (cm^{-1})	B^{cal} (cm^{-1})
(0 2 0)	1041.293	1041.655	0.20356	0.203
(1 2 0)	1886.948	1887.524	0.20305	0.203
(0 4 0)	2099.524	2099.699	0.20405	0.204
(2 2 0)	2726.565	2727.243	0.20252	0.202
(1 4 0)	2932.217	2932.587	0.20357	0.203
(0 2 1)	3088.908	3088.971	0.20238	0.202
(0 6 0)	3165.801	3165.826	0.20444	0.204
(3 2 0)	3560.106	3560.799	0.20198	0.202
(2 4 0)	3759.657	3760.118	0.20308	0.203
(1 2 1)	3931.301	3931.692	0.20192	0.202
(1 6 0)	3985.768	3985.888	0.20396	0.204
(0 4 1)	4134.903	4134.869	0.20293	0.203
(0 8 0)	4238.101	4238.080	0.20477	0.205
(4 2 0)	4387.525	4388.176	0.20142	0.201
(3 4 0)	4581.741	4582.210	0.20257	0.202
(2 2 1)	4767.612	4768.196	0.20146	0.201
(2 6 0)	4801.269	4801.416	0.20346	0.203
(1 4 1)	4964.275	4964.577	0.20245	0.202
(1 8 0)	5045.220	5045.172	0.20428	0.204
(0 2 2)	5113.391	5113.394	0.20121	0.201

Table 6 (*continued*)

$(v_1\, v_2\, v_3)$	E_n^{obs} (cm^{-1})	E_n^{cal} (cm^{-1})	B^{obs} (cm^{-1})	B^{cal} (cm^{-1})
(0 6 1)	5190.281	5190.279	0.20336	0.203
(5 2 0)	5208.770	5209.353	0.20084	0.201
(0 10 0)	5314.913	5314.982	0.20503	0.205
(4 4 0)	5398.381	5398.798	0.20205	0.202
(3 2 1)	5597.630	5598.271	0.20107	0.201
(3 6 0)	5612.327	5612.476	0.20286	0.203
(2 4 1)	5788.391	5788.887	0.20204	0.202
(2 8 0)	5848.571	5848.482	0.20379	0.204
(1 2 2)	5952.266	5952.703	0.20081	0.201
(1 6 1)	6006.877	6007.087	0.20289	0.203
(6 2 0)	6023.775	6024.300	0.20023	0.200
(1 10 0)	6109.013	6108.944	0.20453	0.204
(0 4 2)	6147.197	6147.178	0.20182	0.202
(5 4 0)	6209.497	6209.826	0.20151	0.201
(0 8 1)	6252.586	6252.765	0.20372	0.204
(0 12 0)	6394.970	6395.277	0.20524	0.205
(4 6 0)	6416.182	6416.265	0.20226	0.202
(4 2 1)	6423.958	6424.599	0.20065	0.200
(3 4 1)	6607.130	6607.695	0.20160	0.201
(3 8 0)	6647.907	6647.775	0.20329	0.203
(2 2 2)	6785.024	6785.745	0.20042	0.200
(2 6 1)	6819.093	6819.413	0.20240	0.202
(7 2 0)	6832.463	6832.988	0.19960	0.199
(2 10 0)	6900.078	6899.921	0.20404	0.204
(1 4 2)	6973.126	6973.585	0.20143	0.201
(6 4 0)	7015.011	7015.245	0.20095	0.201
(1 8 1)	7056.022	7056.239	0.20324	0.203
(0 2 3)	7114.782	7114.908	0.20005	0.200
(1 12 0)	7175.842	7175.948	0.20471	0.205
(0 6 2)	7192.013	7192.180	0.20229	0.202
(5 6 0)	7218.073	7217.977	0.20201	0.202
(5 2 1)	7241.209	7241.885	0.19984	0.200
(0 10 1)	7320.138	7320.643	0.20404	0.204
(4 4 1)	7420.293	7420.786	0.20118	0.201
(4 8 0)	7443.151	7443.024	0.20273	0.203
(0 14 0)	7477.159	7477.868	0.20541	0.205
(3 2 2)	7611.333	7612.174	0.20016	0.200
(3 6 1)	7627.092	7627.470	0.20177	0.202
(8 2 0)	7634.740	7635.395	0.19895	0.199
(3 10 0)	7687.720	7687.522	0.20355	0.203
(2 4 2)	7793.796	7794.552	0.20103	0.201
(7 4 0)	7814.845	7815.013	0.20036	0.200
(2 8 1)	7855.851	7856.072	0.20276	0.203
(1 2 3)	7949.866	7950.525	0.19972	0.199
(2 12 0)	7954.508	7954.508	0.20423	0.204
(1 6 2)	8005.130	8005.620	0.20183	0.202
(6 6 0)	8014.089	8013.876	0.20149	0.201
(6 2 1)	8053.147	8053.774	0.19927	0.199

[a] The observed values are taken from Fayt and coworkers [9].

only $-17\,553.99$ cm^{-1}. Figs. 2 and 3 show that although OCS has been known as a typical normal mode type molecule [12], due to strong intermodal couplings, the eigenstates in the vibrationally highly excited region can be significantly deformed from normal mode type.

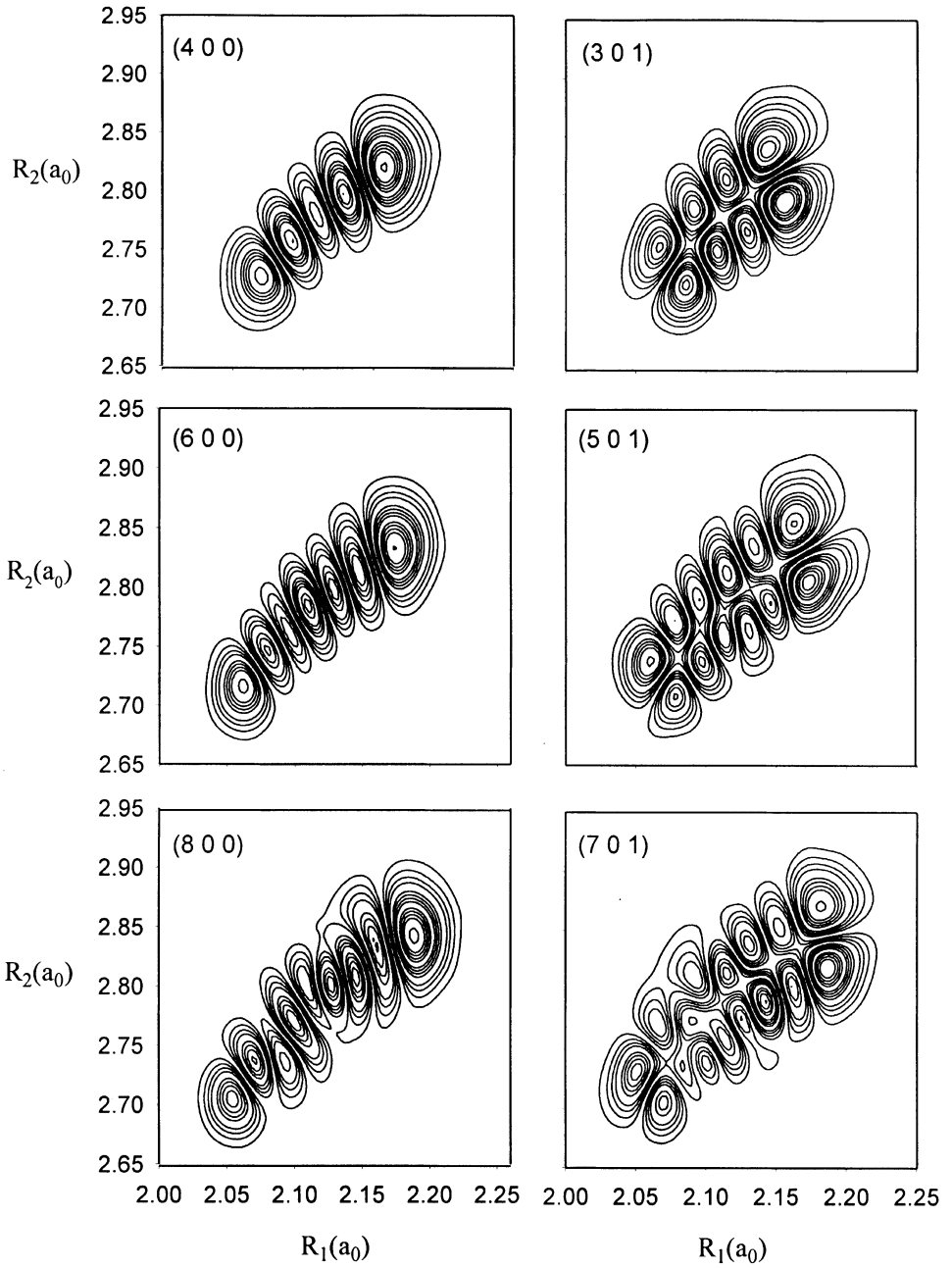

Fig. 2. Contour plots of vibrational eigenfunctions (4 0 0), (3 0 1), (6 0 0), (5 0 1), (8 0 0) and (7 0 1) of OCS in Radau coordinates, with the Radau angle is fixed at the equilibrium value.

In this work, we refined the PES of OCS by involving the experimental data of the energies of all states up to 8000 cm^{-1} in the optimization of the potential parameters. For the unobserved levels, we used the values calculated by Fayt and coworkers [9] because of their reliability. The cal-

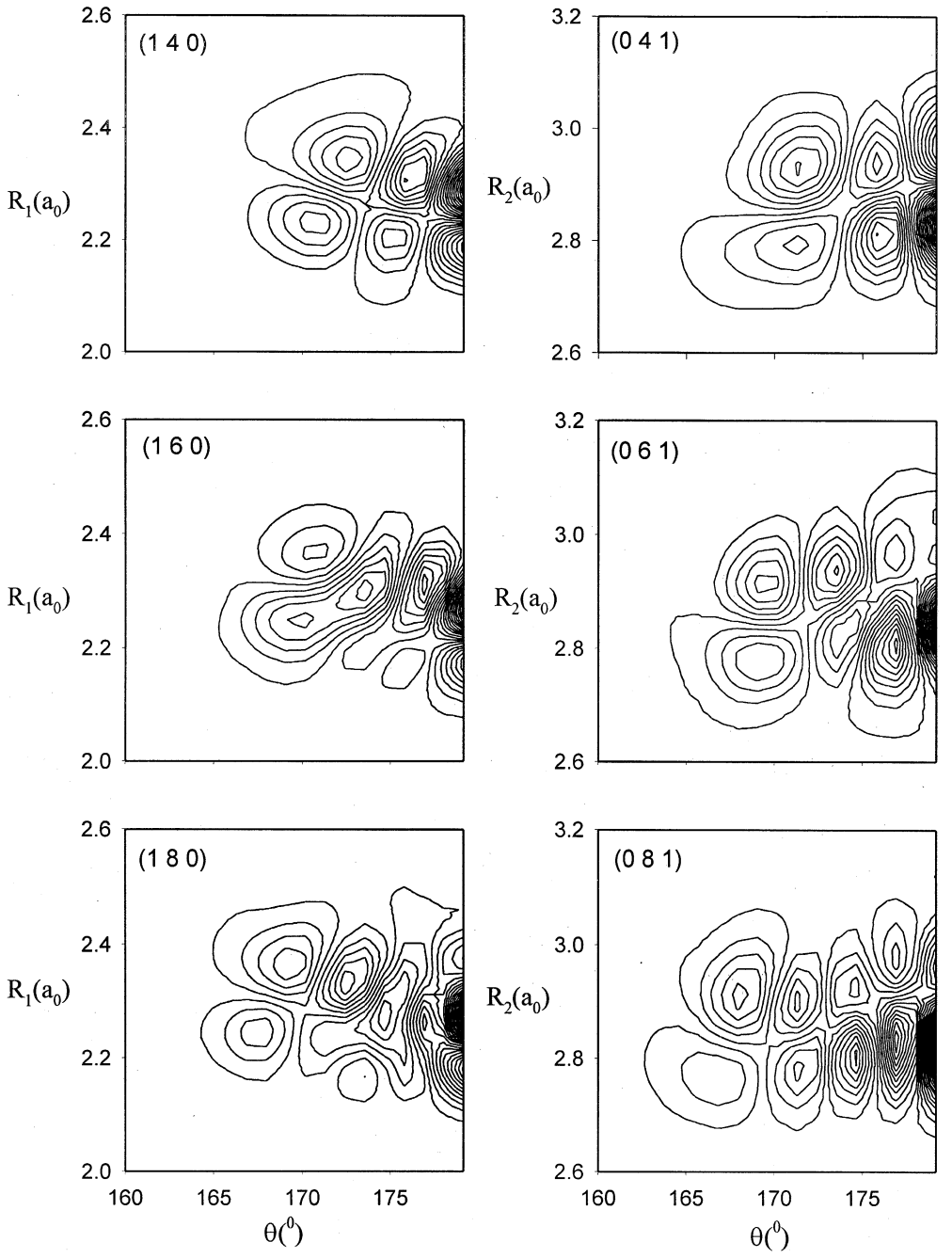

Fig. 3. Contour plots of vibrational eigenfunctions (1 4 0), (0 4 1), (1 6 0), (0 6 1), (1 8 0), and (0 8 1) of OCS in Radau coordinates, with the Radau bond length R_2 (left) and R_1 (right) fixed at the equilibrium value.

culated quartic force constants from the refined potential are very close to the recent high level ab initio calculations [17,18]. We wish this study may provide a new candidate of the potential of

OCS, which could be used in the further theoretical study on this important molecule.

Acknowledgements

This work has been supported by the National Natural Science Foundation of China (grant no. 29892162 and 29973027), by the Special Doctoral Research Foundation of the State Education Commission of China, and by the Sichuan Youth Science and Technology Foundation. We appreciate most gratefully the referee for the very helpful suggestions on the improvement of the manuscript and Prof. Fayt who kindly sent us their calculated vibrational energy levels and effective rotational constants.

References

[1] P.J. Maroulis, A.L. Torres, A.R. Bandy, Geophys. Res. Lett. 4 (1977) 510.
[2] K.B. Jefferts, A.A. Penzias, R.W. Wilson, P.M. Solomon, Astrophys. J. 168 (1971) L111.
[3] P.M. Solomon, A.A. Penzias, K.B. Jefferts, R.W. Wilson, Astrophys. J. 185 (1973) L63.
[4] E.A. Triaille, C.P. Courtoy, J. Mol. Spectrosc. 18 (1965) 118.
[5] A. Fayt, R. Vandenhaute, J.G. Lahaye, J. Mol. Spectrosc. 119 (1986) 233.
[6] J.G. Lahaye, R. Vandenhaute, A. Fayt, J. Mol. Spectrosc. 123 (1987) 48.
[7] A. Belafhal, A. Fayt, G. Guelachvili, J. Mol. Spectroc. 174 (1995) 1.
[8] C. Hornberger, B. Boor, R. Stuber, W. Demtroder, S. Naim, A. Fayt, J. Mol. Spectrosc. 179 (1996) 237.
[9] E. Rbaihi, A. Belafhal, J.V. Auwera, S. Naim, A. Fayt, J. Mol. Spectrosc. 191 (1998) 32.
[10] S. Naim, A. Fayt, H. Bredohl, J.-F. Blavier, I. Dubois, J. Mol. Spectrosc. 192 (1998) 91.
[11] T. Strugariu, S. Naim, A. Fayt, H. Bredohl, J.-F. Blavier, I. Dubois, J. Mol. Spectrosc. 189 (1998) 206.
[12] S. Tranchart, I.H. Bachir, T.R. Huet, A. Olafsson, J.-L. Destombes, S. Naim, A. Fayt, J. Mol. Spectrosc. 196 (1999) 265.
[13] Y. Morino, T. Nakagawa, J. Mol. Spectrosc. 26 (1968) 496.
[14] A. Foord, J.G. Smith, D.H. Whiffen, Mol. Phys. 29 (6) (1975) 1685.
[15] D. Steele, W.B. Person, K.G. Brown, J. Phys. Chem. 85 (1981) 2007.
[16] K.A. Peterson, R.C. Mayrhofer, R.C. Woods, J. Chem. Phys. 94 (1) (1991) 431.
[17] J.M.L. Martin, J.-P. Francois, R. Gubels, J. Mol. Spectrosc. 169 (1995) 445.
[18] Y. Pak, R.C. Woods, J. Chem. Phys. 107 (13) (1997) 5094.
[19] A. Hishikawa, K. Ohde, R. Itakura, S. Liu, K. Yamanouchi, K. Yamashita, J. Phys. Chem. A 101 (1997) 694.
[20] J. Zuniga, A. Bastida, M. Alacid, A. Requena, J. Chem. Phys. 113 (2000) 5695.
[21] C.R. Bailey, A.B.D. Cassie, Proc. R. Soc. London 135 (1932) 375.
[22] D. Xie, G. Yan, Science in China B 39 (1996) 439.
[23] P. Jensen, J. Mol. Spectrosc. 128 (1988) 478.
[24] G. Yan, D. Xie, A. Tian, J. Phys. Chem. 98 (1994) 8870.
[25] B.R. Johnson, W.P. Reinhardt, J. Chem. Phys. 85 (1986) 4538.
[26] J. Echave, D.C. Clary, Chem. Phys. Lett. 190 (1992) 225.
[27] R. Chen, H. Guo, Chem. Phys. Lett. 277 (1997) 199.
[28] G.C. Groenenboom, H.M. Buck, J. Chem. Phys. 92 (1990) 4374.
[29] C.C. Paige, J. Inst. Math. Appl. 10 (1972) 373.
[30] C.C. Paige, J. Inst. Math. Appl. 18 (1976) 341.
[31] J.K. Cullum, R.A. Willoughby, Lanczos Algorithms for Large Symmetric Eigenvalue Computations, vol. I, Birkhauser, Boston, 1985.
[32] G. Ma, R. Chen, H. Guo, J. Chem. Phys. 110 (1999) 8408.
[33] I.M. Mills, A.G. Robiette, Mol. Phys. 56 (1985) 743.
[34] B.R. Johnson, J. Chem. Phys. 67 (1977) 4086.
[35] A. Fayt, private communication, 2001.
[36] B. Frech, M. Murtz, P. Palm, R. Lotze, W. Urban, A.G. Maki, J. Mol. Spectrosc. 190 (1998) 91.